

# Stability Control Method of Hybrid AC-DC Transmission Systems Considering Cross-region Multi-Energy Coordination

Peng Sun, Yun Teng, *Member, IEEE*, Ouyang Leng, Zhe Chen, *Fellow, IEEE*.

**Abstract**—China has built the largest hybrid AC-DC power systems with the highest voltage level in the world. How to effectively guarantee the stable operation of the hybrid AC-DC power systems is an urgent theory and technical demand. In view of the stability problem of hybrid AC-DC transmission systems with high share of wind power, a hybrid AC-DC transmission systems stability control method that considers cross-region multi-energy coordination is established in this paper. Aiming at the uncertainty of high share of wind power, the dynamic inversion method is used as the inner loop of robust control, and the battery energy storage and regenerative electric boiler are used as multiple energy sources to coordinate, and the outer loop robust control is performed for uncertainty compensation. The hybrid AC-DC weak-sending terminal system with wind power is analyzed and designed by  $\mu$ -synthesis based on the  $H_\infty$  control, and a stability control method of the hybrid AC-DC transmission systems considering cross-region multi-energy coordination is established. Simulation results show that the model proposed in this paper can guarantee the robustness of the dynamic inversion method and improves the control performance of AC-DC transmission systems.

**Index Terms**—AC-DC transmission system; uncertainty; multi-energy coordination; robust control

## I. INTRODUCTION

Hybrid AC-DC power systems are new form of power grid development, which have the characteristics of vulnerability, controllability, and cascading failures [1-3]. China has built the largest hybrid AC-DC power systems with the highest voltage level in the world, and large-scale UHV (Ultra High Voltage) hybrid AC-DC power systems are in a period of rapid development [4-6]. However, the control natures of AC and DC systems are different, and the hybrid AC-DC power systems after fault has the characteristics of time-space non-linear and time-varying characteristics [7-9]. The conventional AC system fault analysis method based on Thevenin's equivalent circuit can not effectively evaluate its

This work was supported by the National Key Research and Development Program of China (No.2017YFB0902100).

Peng Sun, Yun Teng are with Shenyang University of Technology, Shenyang 110870, China. (Corresponding author: Yun Teng. e-mail: [tengyun@sut.edu.cn](mailto:tengyun@sut.edu.cn)).

Ouyang Leng is with the State Grid East Inner Mongolia Economic Research Institute, Huhhot 010020, China.

Zhe Chen is Department of Energy Technology, Aalborg University, Aalborg, DK DK 9220.

DOI: 10.17775/CSEEJPES.2020.00510

transient process, and it's urgent to find a new method for transient stability control of hybrid AC-DC power systems.

Hybrid AC-DC power systems with high share of renewable energy are accompanied by many uncertain parameter perturbations, such as wind power, load and other uncertainties. If transient faults occur at the same time, the entire system may be unstable, which may bring severe challenges to the stability control of hybrid AC-DC transmission systems.

The stable control of hybrid AC-DC power systems is a crucial research field, and it is an effective guarantee for the stable operation and sustainable use of energy [10-12]. Among them, the AC subsystem and the DC subsystem are interconnected through DC/AC converter stations, power electronic transformers and other equipments [13]. At present, scholars have many mature researches on the stability control of AC subsystem or the stability control of DC subsystem [14-17]. Different from a single AC subsystem or a DC subsystem, the hybrid AC-DC power systems operate in a more complex mode, with strong non-linearity, time variability, and uncertainty [18-19]. On the one hand, the interconnection of converter stations when the system is grid-connected or isolated, and the equipment needs to keep the AC and DC subsystems working properly. On the other hand, under different operating modes, especially when the island is operating without the support of the distribution network, the converter station and the source network load and storage need to cooperate with each other to formulate an appropriate control strategy.

In recent years, scholars have gradually paid more attention to the safety and stability control of UHV power grids. A flexible voltage control strategy considering high share of energy storage was proposed in [20] to improve the inertial response of the DC grid to the AC grid. The DC power modulation of a multi-machine hybrid AC-DC power systems is designed in [21-22] to improve the transient stability of the system. At present, research on the transient stability control of delivery systems for high share of wind power access is in its infancy. The wind-fire power angle curve is used as the active crossover in [23], but the fast recovery characteristics of doubly-fed wind turbines are not conducive to the stability of the system's power angle. Wind power has advantages and disadvantages for AC-DC interconnection systems due to the uncertainty of wind-fire interaction [24-25]. The current research rarely involves the transient stability optimization control of hybrid AC-DC power systems with weak

transmitting end high power and high uncertainty wind power.

Hybrid AC-DC microgrids can meet both AC and DC load requirements, which are considered to be the preferred mode for efficient development and utilization of distributed energy in the future[26-27]. A coordinated control strategy for bidirectional AC-DC converters in a hybrid microgrid in island operation mode is proposed in [28-29], but an energy management system was required to determine its operating mode based on the measured converter power value. To address the intrinsically stochastic availability of high share of renewable energy in hybrid AC-DC microgrids, a novel power scheduling approach is introduced in[30], which involves the actual renewable energy as well as the energy traded with the main grid. A robust optimal power management system is developed in [31-32] for a hybrid AC-DC micro-grid, where the power flow in the micro-grid is supervised based on solving an optimization problem.

This paper takes the actual project of hybrid AC-DC power systems to realize wind power transmission as an example, and a stable control method of hybrid AC-DC power systems considering wind power uncertainty is proposed. In Section II, based on the structured and unstructured uncertainty characteristics of hybrid AC-DC transmission systems, a linear fractional transformation (LFT) model for uncertainty of hybrid AC-DC power systems is proposed. In Section III, the battery energy storage and regenerative electric boiler models are simply analyzed. In Section IV, the dynamic inversion method is used as the inner loop of robust control, the outer loop robust control compensation is performed for model uncertainty. Based on this, a hybrid AC-DC controller model based on dynamic inversion and  $H_\infty$  robust control is established. In Section V, Take the actual project of weak transmission end of a hybrid AC-DC power systems in Northeast China as an example. Finally, Section VI summarizes the main outcome of this paper.

## II. UNCERTAINTY MODEL OF AC-DC HYBRID SYSTEM

### A. Structured parameter uncertainty

Errors in specific parameters in hybrid AC-DC power systems represent structured uncertainty. The parameters affecting the structural uncertainty of AC-DC hybrid systems are mainly manifested in wind power, load disturbance, AC line power oscillation, and DC line power oscillation. These four parameters are used as system uncertain parameters. In order to conduct  $\mu$ -analysis later, the standard of uncertain parameters  $\delta$  is normalized into  $\delta'$ :

$$\delta = \frac{\delta^+ + \delta^-}{2} + \frac{\delta^+ - \delta^-}{2} \delta' \quad (1)$$

Where,  $\delta \in [\delta^-, \delta^+]$ ,  $\delta' \in [-1, 1]$ . In this way, the uncertain parameters are divided into two parts: the nominal part and the perturbed part.

### B. Unstructured uncertainty

The situation where the parameter perturbation and the actual structure between the systems are unknown is called unstructured uncertainty, and it can be divided into two types:

additive and product. Assuming that the nominal parameter of uncertainty variable is  $N$  and errors is  $\Delta$ , and weighting terms  $W_1, W_2$  to measure the error term, then the uncertainty term can be expressed by  $\Delta W_1 \Delta W_2$ . In the new system, the additive uncertainty and product uncertainty are expressed as,  $\Pi = N + \Delta W_1 \Delta W_2$ ,  $\Pi = (1 + \Delta W_1 \Delta W_2)N$ , respectively.

### C. LFT uncertainty Modeling

Linear fractional transformation (LFT) of structural and non-structural uncertainties  $\underline{\Delta}$  is performed in scalar and full form:

$$\underline{\Delta} = \text{diag}(\delta_1 I_{r_1}, \delta_2 I_{r_2}, \dots, \delta_s I_{r_s}, \Delta_1, \Delta_2, \dots, \Delta_F) \quad (2)$$

Where,  $\delta_i \in C$ ,  $\Delta_j \in C^{m_j \times m_j}$ ,  $1 \leq i \leq S$ ,  $1 \leq j \leq F$ .  $\delta_i$  and  $\Delta_j$  represent structural uncertain parameters and non-structural uncertainty blocks, respectively;  $r_i$  is the dimension of scalar uncertainty, and  $m_j$  is the dimension of full uncertainty. The LFT has two forms of upper LFT and lower LFT, and the corresponding calculation formula is

$$F_u(M, \underline{\Delta}) = M_{22} + M_{21} \underline{\Delta} (I - M_{11} \underline{\Delta})^{-1} M_{12} \quad (3)$$

$$F_l(M, \underline{\Delta}) = M_{11} + M_{12} \underline{\Delta} (I - M_{22} \underline{\Delta})^{-1} M_{21} \quad (4)$$

$$M = \begin{bmatrix} M_{11} & M_{12} \\ M_{21} & M_{22} \end{bmatrix} \quad (5)$$

Where, eqn (3) is the upper LFT form, eqn (4) is the lower LFT form, and  $M$  is the corresponding variable parameter of the system.

Uncertainty can generally be described by structural uncertain parameters, but at this time the parameter perturbation is linear. If the parameter perturbation is non-linear, it can be expressed as an  $m$ -degree order polynomial function  $N(\delta) = a_0 + a_1 \delta + \dots + a_m \delta^m$  of  $\delta$ . After ignoring the higher-order small terms of order 3 and above, set  $\delta_1 = \delta$ ,  $\delta_2 = \delta^2$ , then  $N(\delta) = F_l(X, \delta I)$ , in this way, the non-linear part becomes linear. Where

$$X = \begin{bmatrix} a_0 & a_1 & a_2 \\ 1 & 0 & 0 \\ 0 & 1 & 0 \end{bmatrix} \quad (6)$$

In addition, it is necessary to expand the terms related to the uncertain parameter  $A_0 + \sum \delta_i A_i$  in the system, and ignore the higher-order terms into  $B_0 + \sum \delta_i B_i$ . The structured uncertainty can be expressed as

$$\begin{bmatrix} \dot{x} \\ y \end{bmatrix} = \begin{bmatrix} A_0 + \sum_{i=1}^m \delta_i A_i & B_0 + \sum_{i=1}^m \delta_i B_i \\ C_0 + \sum_{i=1}^m \delta_i C_i & D_0 + \sum_{i=1}^m \delta_i D_i \end{bmatrix} \begin{bmatrix} x \\ u \end{bmatrix} \quad (7)$$

$$\left( \begin{bmatrix} A_0 & B_0 \\ C_0 & D_0 \end{bmatrix} + \sum_{i=1}^m \delta_i \begin{bmatrix} A_i & B_i \\ C_i & D_i \end{bmatrix} \right) \begin{bmatrix} x \\ u \end{bmatrix}$$

Where,  $A_i \in R^{n \times n}$ ,  $B_i \in R^{n \times n_u}$ ,  $C_i \in R^{n_y \times n}$ ,  $D_i \in R^{n_y \times n_u}$ .

If the uncertain term is used as the denominator, it can be transformed into a product form by fractional transformation. The structured uncertain LFT model can be obtained by decomposing the perturbation matrices  $A_i, B_i, C_i, D_i$ . The standardization of unstructured uncertainty is the same as that

in [33]. In this way, the LFT uncertainty model of the AC-DC hybrid transmission system is established.

### III. MODEL OF BATTERY ENERGY STORAGE AND REGENERATIVE ELECTRIC BOILER

#### A. Battery energy storage

The state-of-charge(SOC) model of battery energy storage is as follows

$$SOC(t) = [E_{BES}(t-1) + (\eta_{EI}P_{EI}(t) - P_{EO}(t) / \eta_{EO})\Delta t] / E_{BES,max} \quad (8)$$

Where,  $E_{BES}(t)$  is the battery capacity at time  $t$ ;  $P_{EI}(t)$  and  $P_{EO}(t)$  are the battery storage power at time  $t$ ;  $\eta_{EI}, \eta_{EO}$  are the battery storage and discharge efficiency;  $\Delta t$  is the operation period.  $E_{BES,max}$  is the total energy that can be stored in the battery.

#### B. Regenerative electric boiler

Regenerative electric boiler consists of electric heating unit and heat storage unit:

$$\begin{cases} P_{EB,h}(t) = P_{EB,e}(t)\eta_{EB} \\ SOH(t) = [E_{EB}(t-1) + (P_{EB,h}(t) - P_{HO} / \eta_{HO})\Delta t] / E_{HS,max} \end{cases} \quad (9)$$

Where,  $P_{EB,h}(t)$ ,  $P_{EB,e}(t)$  are the power consumption and heating power of the electric boiler;  $\eta_{EB}$  is the electro-thermal conversion efficiency;  $E_{EB}(t)$  is the heat storage capacity at time  $t$ ;  $P_{HO}(t)$  is the heat release power at time  $t$ ;  $\eta_{HO}$  is heat release efficiency of heat storage.  $SOH(t)$  is the state of heat of the regenerative electric boiler at time  $t$ .  $E_{HS,max}$  is the total energy that can be stored by the regenerative electric boiler.

In the hybrid AC-DC transmission control system, the power of the battery energy storage and the regenerative electric boiler can be controlled according to the SOC of the battery energy storage and the SOH of the regenerative electric boiler, and wind power fluctuation can be compensated.

### IV. CONTROL STRATEGY AND CONTROLLER DESIGN

The LFT model of uncertainty is applied to the hybrid AC-DC control system. The controller uses a combination of inner loop dynamic inversion control and outer loop robust control to guarantee the stable operation and robustness of the system. The hybrid AC-DC control system designed in this paper is shown in Fig. 1. The inner loop is composed of a dynamic inversion fast loop and a hybrid AC-DC nonlinear model. The outer loop is a fast loop robust controller.

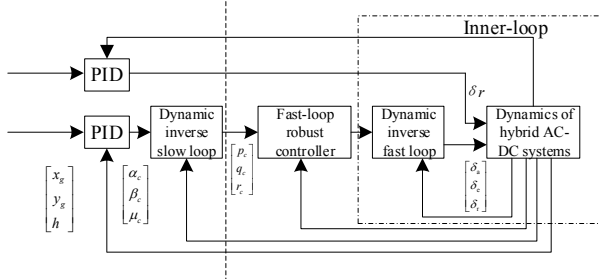


Fig. 1 Hybrid AC-DC transmission control system structure

The dynamic inversion inner loop can cancel the nonlinear term of the model, so the closed loop system of the inner loop presents a linear system characteristic. The perturbed part mainly manifests as system uncertain parameters, structure perturbation and unmodeled errors. In order to avoid directly using the high-order controller brought by  $H_\infty$  robust control, an outer-loop robust controller with a lower order and fixed structural parameters can be designed.

#### A. Nonlinear dynamic inversion control law --- inner loop

The dynamic inversion method is a control method for decoupling the coupled quantities. In this paper, the nonlinear term is used for dynamic inversion design of the inner loop. The equation of state in the nonlinear equation of the hybrid AC-DC transmission system is:

$$\begin{cases} \dot{x} = f(x) + g(x)u \\ y = h(x) \end{cases} \quad (10)$$

Where,  $x \in R^n$  is the state quantity of the hybrid AC-DC power systems, such as active and reactive power in each regional power grid, and SOC of battery energy storage and SOH of regenerative electric boiler;  $u \in R^p$  is the control quantity, which is the variable parameter of the control system such as the motor rotor speed, power angle and power of energy storage;  $y \in R^m$  are the active and reactive output of hybrid AC-DC transmission system. The dynamic inversion of the system can be obtained by taking the derivative of the output  $y$  until  $u$  appears in the result. Moreover, assuming that  $g(x)$  is invertible for all values of  $x$ , the control law can be obtained by the algebraic inverse method to select the appropriate input  $u$ .

If  $p=m$ , the control law can be written as:

$$u = \left[ \frac{\partial CV}{\partial x} g_m(x) \right]^{-1} \left[ C\dot{V}_d - \frac{\partial CV}{\partial x} f_m(x) \right] \quad (11)$$

Where,  $g_m$  is a dynamic model;  $f_m$  is a control distribution function;  $CV(x)$  and  $C\dot{V}_d$  are a function of state variable and a desired control command, respectively. If the hybrid AC-DC power systems model is accurate, then  $g_m=g$ ,  $f_m=f$ . When  $y=x$ , i.e., when the output quantity is equal to the state quantity,  $y=\dot{x}=f(x)+g(x)u$ , the closed loop becomes  $\dot{y}=\dot{x}=C\dot{V}_d$ . Set  $C\dot{V}_d=K_c(x_c-x)$ ,  $x_c$  and  $K_c$  are the desired output and band bandwidth, respectively. The control inputs of the fast loop are:

$$\begin{bmatrix} \delta_a \\ \delta_e \\ \delta_r \end{bmatrix} = g^{-1}(x) \left( \begin{bmatrix} \dot{p}_d \\ \dot{q}_d \\ \dot{r}_d \end{bmatrix} - \begin{bmatrix} f_p(x) \\ f_q(x) \\ f_r(x) \end{bmatrix} \right) \quad (12)$$

Where,  $\delta_a, \delta_e, \delta_r$  are 3 units of hybrid AC-DC transmission systems, AC section, DC section and energy storage.

#### B. $H_\infty$ control and NDI --- outer loop

The  $H_\infty$  control problem of hybrid AC-DC system can be expressed as:

$$N = \begin{bmatrix} N_{11} & N_{12} \\ N_{21} & N_{22} \end{bmatrix} = \begin{bmatrix} A & B_1 & B_2 \\ C_1 & D_{11} & D_{12} \\ C_2 & D_{21} & D_{22} \end{bmatrix} \quad (13)$$

Where,  $N$  is the object of augmentation.

The fast loop closed loop formed by the dynamic inversion method, the input is the power command of the hybrid AC-DC power system, and the output is the active and reactive output of each unit. In an ideal state, the object  $G_{inner-loop}$  is a decoupling integral system in the form of a  $3 \times 3$  matrix. It needs to be augmented into  $N_{outer-loop}$  and added to the outer loop  $H_\infty$  control.

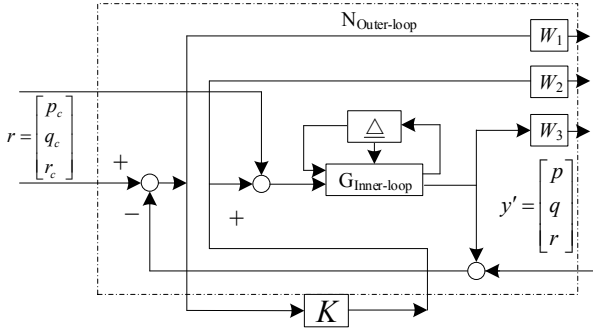


Fig. 2 Outer loop of control system and augmentation of uncertainty for hybrid AC-DC transmission systems

Fig. 2 shows the outer loop of control system and augmentation of uncertainty for hybrid AC-DC transmission systems. In the figure,  $r$  is the control command on the hybrid AC-DC transmission control system;  $n$  and  $d$  are noise and disturbance respectively;  $W_1, W_2, W_3$  are third-order weight function matrices.

After adding the uncertainty to the augmented mode, the state space of  $N_{outer-loop}$  can be expressed as:

$$N_{outer-loop} = \begin{bmatrix} N_{11} & N_{12} \\ N_{21} & N_{22} \end{bmatrix} = \begin{bmatrix} A + \Delta A & B_1 & B_2 + \Delta B_2 \\ C_1 & D_{11} & D_{12} \\ C_2 & D_{21} & D_{22} \end{bmatrix} \quad (14)$$

C. System robust stability and  $\mu$ - $H_\infty$  controller

For general unstructured disturbances, stability can be achieved by  $H_\infty$  controller (such as loop forming  $H_\infty$  control), but for some elements with structured disturbances, it cannot be taken into account. The controller is conservative, and the stability and robustness of the system cannot be easily guaranteed with structural disturbances.

Zhou et al. [34] gave the internal stability conditions required by the control structure similar to Figure 1, and transformed them into  $\mu$  boundary value conditions to unify the robust stability and robust performance. It is pointed out that stability is not the only property that a closed-loop system must be robust to perturbation. When there is perturbation, the influence of interference on tracking and adjustment errors will be greatly enhanced. In most cases, long before instability occurs, the closed-loop performance will deteriorate to an unacceptable level. Therefore, the worst-case parameter analysis of robust performance is also needed.

It is difficult to obtain the  $\mu$  value according to the definition of  $\mu$  value. The D-K iterative method [35] can be used to approximate the  $\mu$  boundary of the system. Although the  $\mu$  boundary obtained by this method is not accurate, but it has great value in practical applications.

According to the system model corresponding to the inner loop dynamic inversion method, its uncertainty includes 4 uncertain parameters  $\delta_1, \delta_2, \delta_3, \delta_4$  with a dimension of  $1 \times 1$ .

There are two  $3 \times 3$  non-structured uncertain blocks  $\Delta_1$  and  $\Delta_2$  at the input and output. Therefore,  $\underline{\Delta} = \text{diag}(\delta_1, \delta_2, \dots, \delta_4, \Delta_1, \Delta_2)$ . The  $H_\infty$  augmented uncertain system model has 12 inputs and 12 outputs, and the closed-loop feedback loops  $p, q, r$  form a  $3 \times 3$  feedback matrix. Matlab's robust control toolbox provides a graphical user interface for  $\mu$  calculations. After calling this interface for 5 iterations, the  $\mu$  value is stable at about 0.91, which meets the condition of robust stability  $\mu < 1$ .

V. SIMULATION

Take the four-region hybrid AC-DC power system in Fig. 3 as an example for simulation. The equivalent load of the G2 grid is 1200MW, and the equivalent loads of the three regional grids of G1, G3, and G4 are 2200MW. The installed capacity of G2 is 2400MW, including 1300MW of wind power. The installed capacity of G2, G3 and G4 regions is 1600MW, 1600MW and 1400MW. Four regions have 300MW of power storage and 200MW of heat storage. Under the stable operating conditions of the rated parameters, the wind power transmitted by Line 1, Line 2 and Line 4 are: 500MW, 400MW and 400MW. Tab.I shows some simulation system parameters.

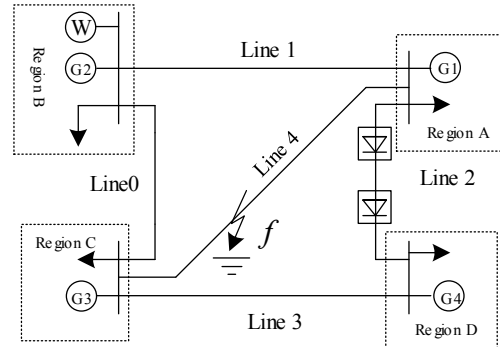


Fig. 3 Structure of hybrid AC-DC power system

TABLE I  
SIMULATION SYSTEM PARAMETERS

Parameter Type	parameter settings
DC line power	1000 MW
Rated DC voltage	$\pm 500$ kV
Rated DC current	2 kA
AC line voltage	500 kV

A. Simulation analysis of response characteristics of transient stability control strategy

Fig. 4 is a singular value curve diagram of the sensitivity function SF (a) and the complementary sensitivity function CSF (b) after taking into account the uncertainty factor of the hybrid AC-DC transmission control system by  $\mu$ - $H_\infty$  control.  $SF = (I + N_{outer-loop} K_{\mu-H_\infty})^{-1}$ ,  $CSF = N_{outer-loop} K_{\mu-H_\infty} (I + N_{outer-loop} K_{\mu-H_\infty})^{-1}$ , the solid line represents the design state point, and the circle line represents the state point. It can be seen from the Fig. 4 that for the two state points of hybrid AC-DC hybrid systems, when the uncertainty perturbation is taken into account, the amplitude of SF in the low frequency band is small, thereby maintaining the system's anti-interference ability; The amplitude decays quickly, which can maintain the uncertainty



suppression ability of the system. The deviation of the amplitude of SF and CSF from the design state point has increased, but it is still within the allowable range.

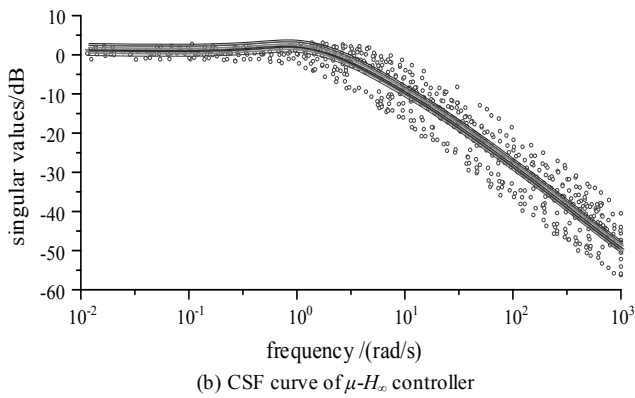
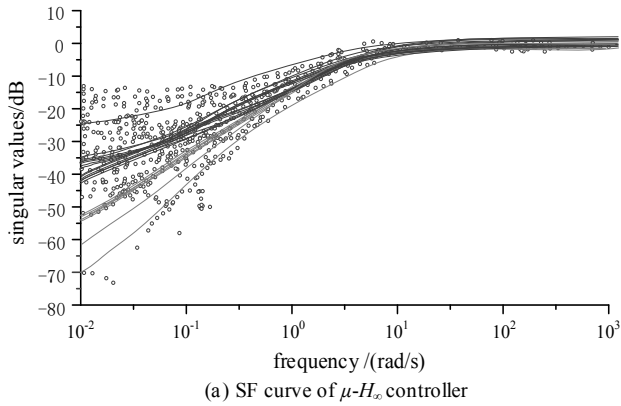


Fig. 4 Closed-loop singular values with uncertainty using  $\mu-H_\infty$  controller

Fig. 5 shows the singular value curve of the sensitivity function and the complementary sensitivity function when the system is in two state points, using the controller of [31]. Compared with Fig. 4, it can be seen that the controller of [31] has a certain stability for parameter perturbation. However, when the parameter changes greatly, the control effect of the  $\mu-H_\infty$  controller designed in this paper is better than that of [31].

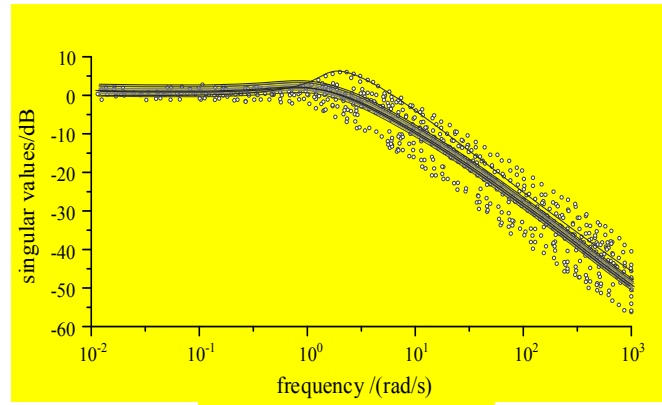
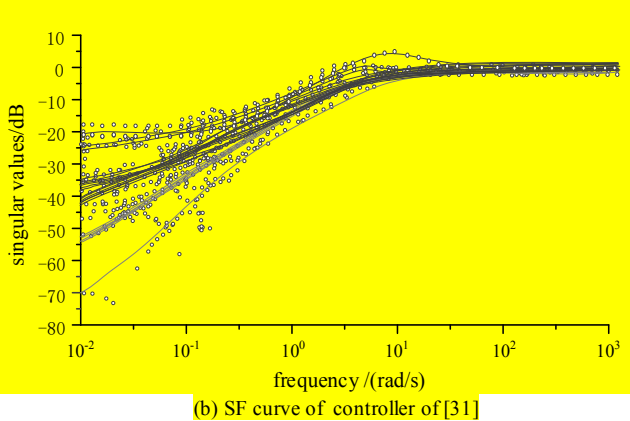


Fig. 5 Closed-loop singular values with uncertainty using  $\mu-H_\infty$  controller

### A. Transient Stability Control Strategy Response Characteristic Simulation Analysis

To verify the robustness of the control strategy, a 20% wind power output uncertainty is added when the system experiences large disturbances. The system power balance control response is shown in Fig. 6.

It can be seen from Fig. 6 that when the power control command of the interconnected system is issued, the lag in the power response will cause a delay in the power response. Under the uncertainty of wind power, the response of the system can track the reference command well. The adjustment time does not exceed 2s, which has good robustness and tracking performance.

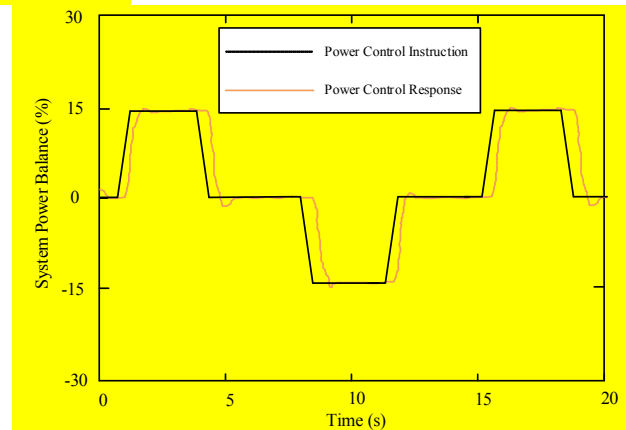


Fig.6 Response of power control under wind power uncertainty.

### B. Simulation analysis of transient stability control performance of interconnected systems

In order to verify the control effect of the LFT robust control method, as compared with the robust controller of the full-order observer (FOO), the weight functions and controller order are the same as the original system.

The initial state of the system is normal operation. A robust controller based on LFT and a robust controller based on FOO are added to the DC rectification side of the four-region interconnected power system [36]. Perturb the system at 0.6s: A three-wire ground short circuit occurs at point f on the AC contact line Line4, which lasts for 0.2s, and the fault is removed

at 0.8s. The stability control of transient process under disturbance is simulated and analyzed.

Assume that the power difference in the system during the fault is 8%. The uncertain parameters set in case 1 are 10%, and the uncertain parameters set in case 2 are 20%. Fig. 7 and Fig. 8 show the change trends of DC power and AC power of the hybrid AC-DC system in case 1 under the two robust controllers.

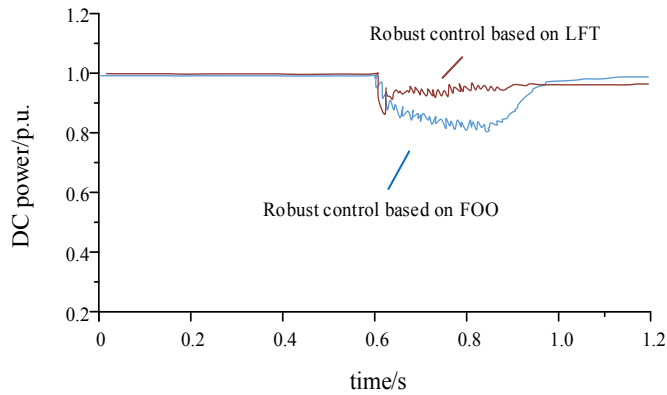


Fig.7 DC Power Control in Transient Process (case 1)

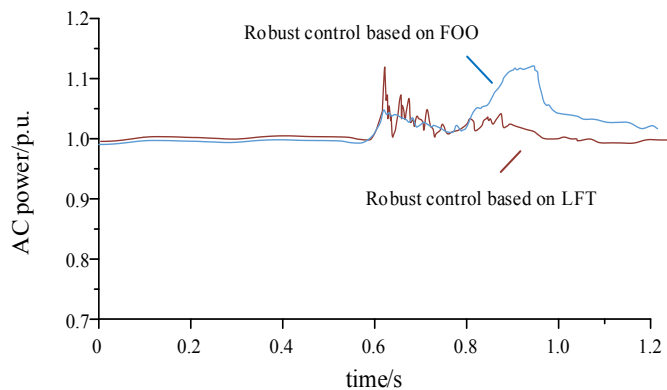


Fig.8 Power Control of AC System During Transient Process (case 1)

During the disturbance process, the communication lines between the grids in the G2 and G4 regions were cut out, and the DC communication lines operated independently. At this time, the outbound wind power from the regional grid G2 to G4 must be transferred to the DC line and other AC lines. Due to the power of the DC channel can't be increased rapidly, which will lead to a greatly increase in the power angle and frequency of the generator in the region 2 of the wind power transmission end, In severe cases, it will cause wind curtailment. If the stability control in the hybrid AC-DC power systems are uncoordinated, the frequency of the system will also be deteriorated, and in severe cases it will cause the system to crash [37].

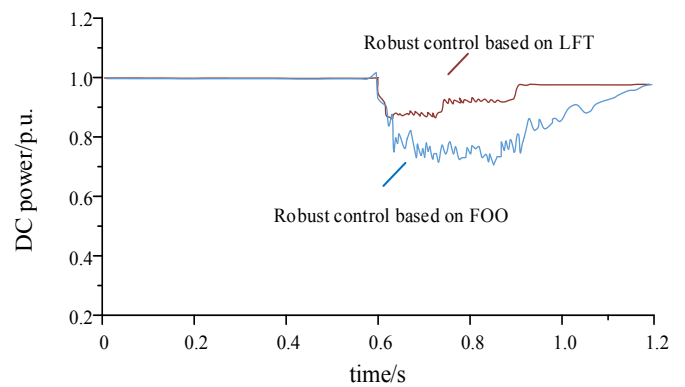


Fig.9 DC Power Control in Transient Process (case 2)

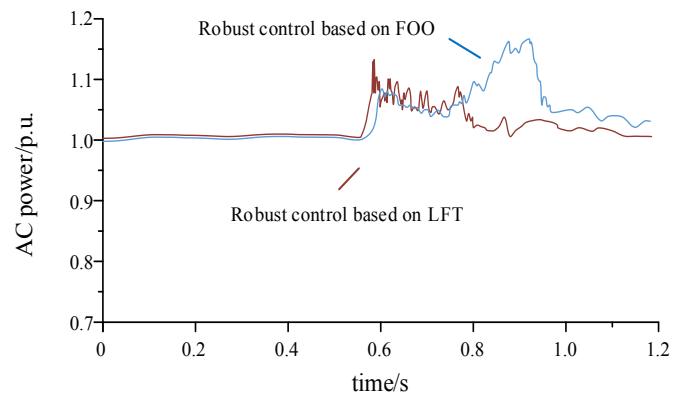


Fig.10 Power Control of AC System During Transient Process (case 2)

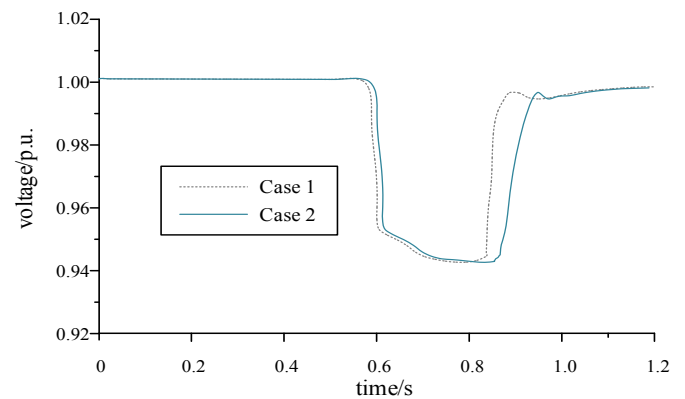


Fig. 11 AC voltage change in Transient Process of two cases under LFT robust control

In order to verify the robustness of the system, the effect of the control strategy was tested in the worst case of the system (case 2, uncertainty 20%). The control effect of the proposed transient stability strategy is shown in Fig. 9 and Fig. 10. The comparison of voltage changes in the two scenarios is shown in Fig. 11.

The robust output feedback control method based on LFT established in this paper makes full use of the short-term overload capacity of the DC wind power transmission channel, and effectively suppresses the power fluctuation in the hybrid AC-DC power systems. In this paper, the dynamic inversion is used as the inner loop, and the inner loop is used as the control object of the outer loop. The comprehensive model with linearization characteristics of the inner loop is subjected to

LFT transformation to establish an uncertain model of the inner loop. By using  $\mu$  synthesis and analysis, the  $\mu$ - $H_\infty$  controller design of the fast loop outer loop is designed. The robustness to the high share of wind power uncertainty and the performance of the transient suppression ability in the hybrid AC-DC power systems can achieve satisfactory results.

## VI. CONCLUSION

In view of the problem of robust optimal control of hybrid AC-DC power systems consisting of multiple regional power grids and containing multiple energy sources, a transient stability control method of hybrid AC-DC transmission systems is proposed, which combines dynamic inversion and robust control based on linear fractional transformation.

1) Based on the structured and unstructured uncertainty characteristics of hybrid AC-DC transmission systems, a linear fractional transformation model for uncertainty of hybrid AC-DC transmission systems is proposed

2) For the linear fractional transformation state equation of hybrid AC-DC transmission systems, a controller model combining the dynamic inversion of transient stability control and  $H_\infty$  robust control is designed.

3) Taking an AC-DC transmission system composed of four regional equivalent grids as an example for simulation analysis, the results show that the control method proposed in this paper has a certain degree of robustness and a good suppression effect on transient processes.

## REFERENCES

- [1] S. Chu, A. Majumdar. "Opportunities and challenges for a sustainable energy future," *nature*, vol. 488, pp. 294, 2012.
- [2] DONG Xinzhou, TANG Yong, BU Guangquan, et al. "Confronting Problem and Challenge of Large Scale AC-DC Hybrid Power Grid Operation," *Proceedings of the CSEE*, no. 39, vol. 11, pp: 3107-3119, Jun, 2019
- [3] X. D. Liang, "Emerging power quality challenges due to integration of renewable energy sources," *IEEE Transactions on Industry Applications*, vol. 53, no. 2, pp. 855-866, Mar./Apr. 2017.
- [4] X. R. Xie, W. Liu, H. Liu, Y. L. Du, and Y. H. Li, "A system-wide protection against unstable SSCI in series-compensated wind power systems," *IEEE Transactions on Power Delivery*, vol. 33, no. 6, pp. 3095-3104, Dec. 2018.
- [5] DENG Wei, WU Zheng, KONG Li, et al. "Coordinated Control Technology for AC/DC Hybrid System," *High Voltage Engineering*, no.10, vol.45, pp 3025-3038, Oct 2019
- [6] BARANWAL M, ASKARIAN A, SALAPAKA S, et al. A distributed architecture for robust and optimal control of DC microgrids[J]. *IEEE Transactions on Industrial Electronics*, 2019, 66(4): 3082-3092.
- [7] Tomasson, Egill, Soder, Lennart. Generation Adequacy Analysis of Multi-Area Power Systems With a High Share of Wind Power[J]. *IEEE Transactions on Power Systems*, no. 33, vol. 4, pp : 3854- 3862. Jul. 2018
- [8] DIAZ N L, LUNA A C, VASQUEZ J C, et al. Centralized control architecture for coordination of distributed renewable generation and energy storage in islanded AC microgrids[J]. *IEEE Transactions on Power Electronics*, 2017, 32(7): 5202-5213.
- [9] AREERAK K, SOPAPIRM T, BOZHKO S, et al. Adaptive stabilization of uncontrolled rectifier based AC-DC power systems feeding constant power loads[J]. *IEEE Transactions on Power Electronics*, 2018, 33(10): 8927-8935.
- [10] Shao Yao, Tang Yong. Fast evaluation of commutation failure risk in multi-infeed HVDC systems[J]. *IEEE Transactions on Power Systems*, 2018, 33(1): 646-653.
- [11] X. Guo, X. Cui, and Q. Lei, "DC short-circuit fault analysis and protection for the overhead line bipolar MMC-HVDC system," *Proceedings of the CSEE*, vol. 37, no. 8, pp. 2177-2184, 2017.
- [12] Bidafar A, Nee H P, Zhang Lidong, et al. Power system stability analysis using feedback control system modeling including HVDC transmission links[J]. *IEEE Transactions on Power Systems*, 2016, 31(1): 116-124.
- [13] Le Blond S, Bertho Jr R, Coury D V, et al. Design of protection schemes for multi-terminal HVDC systems [J]. *Renewable and Sustainable Energy Reviews*, 2016, 56: 965-974.
- [14] Y. Li, L. He, F. Liu, C. B. Li, Y. J. Cao, and M. Shahidehpour, "Flexible voltage control strategy considering distributed energy storages for DC distribution network," *IEEE Transactions on Smart Grid*, vol. 10, no. 1, pp. 163-172, Jan. 2019.
- [15] A. Moawwad, E. F. El-Saadany, and M. S. El Moursi, "Dynamic security-constrained automatic generation control (AGC) of integrated AC/DC power networks," *IEEE Transactions on Power Systems*, vol. 33, no. 4, pp. 3875 - 3885, Jul. 2018.
- [16] Z. Li, Q. R. Hao, F. Gao, L. L. Wu, and M. Y. Guan, "Nonlinear decoupling control of two-terminal MMC-HVDC based on feedback linearization," *IEEE Transactions on Power Delivery*, vol. 34, no. 1, pp. 376-386, Feb. 2019.
- [17] X. Chen, L. Wang, H. S. Sun, and Y. Chen, "Fuzzy logic based adaptive droop control in multiterminal HVDC for wind power integration," *IEEE Transactions on Energy Conversion*, vol. 32, no. 3, pp. 1200 - 1208, Sep. 2017.
- [18] M. A. Abdelwahed and E. F. El-Saadany, "Power sharing control strategy of multiterminal vsc-hvdc transmission systems utilizing adaptive voltage droop," *IEEE Tran. Sustain Energy*, vol. 8, no. 2, pp. 605 - 615, April 2017.
- [19] Y. B. Shu, G. P. Chen, Z. Yu, J. Y. Zhang, C. Wang, and C. Zheng, "Characteristic analysis of UHVAC/DC hybrid power grids and construction of power system protection," *CSEE Journal of Power and Energy Systems*, vol. 3, no. 4, pp. 325-333, Dec. 2017.
- [20] K. Liao and Y. Xu, "A robust load frequency control scheme for power systems based on second-order sliding mode and extended disturbance observer," *IEEE Transactions on Industrial Informatics*, vol. 14, no. 7, pp. 3076 - 3086, Jul. 2018.
- [21] A. Kirakosyan, E. F. El-Saadany, M. S. E. Moursi, S. Acharya, and K. A. Hosani, "Control approach for the multi-terminal hvdc system for the accurate power sharing," *IEEE Transactions on Power Systems*, vol. 33, no. 4, pp. 4323-4334, July 2018.
- [22] Elyas Rakhshani, Pedro Rodriguez. Inertia Emulation in AC/DC Interconnected Power Systems Using Derivative Technique Considering Frequency Measurement Effects[J]. *IEEE Transactions on Power Systems*, 2017, 32(5):3338-3351.
- [23] Gao Shuping, Liu Qi, Song Guobing. Current differential protection principle of HVDC transmission system[J]. *IET Generation, Transmission & Distribution*, 2017, 11(5): 1286-1292.
- [24] Nasri A, Kazempour SJ, Conejo AJ, Ghandhari M. Network-constrained AC unit commitment under uncertainty: a Benders' decomposition approach. *IEEE Trans Power Syst* 2016;31:412-422.
- [25] Samir Irfan, Ashraf Ahmed, Joung-Hu Park, et al. Current-Sensorless Power-Decoupling Phase-Shift Dual-Half-Bridge Converter for DC-AC Power Conversion Systems Without Electrolytic Capacitor[J]. *IEEE Transactions on Power Electronics*, 2017, 32(5):10-3622.
- [26] Guerrero JM, Loh P C, Lee T L, et al. Advanced control architectures for intelligent microgrids—Part II: Power quality, energy storage, and AC/DC microgrids[J]. *IEEE Transactions on Industrial Electronics*, vol. 60, no. 4, pp. 1263-1270, 2013.
- [27] Hosseinzadeh M, Salmasi F R. Robust Optimal Power Management System for a Hybrid AC/DC Micro-Grid[J]. *IEEE Tran. Sustain Energy*, vol. 6, no. 3, pp. 675-687, 2015.
- [28] Li Xialin, Li Guo, Li Yunwei, et al. A unified control for the DC-AC interlinking converters in hybrid AC/DC microgrids[J]. *IEEE Transactions on Smart Grid*, vol. 9, no. 6, pp. 6540-6553, 2018.
- [29] GUERRERO J M, VASQUEZ J C. A distributed control strategy for coordination of an autonomous LVDC microgrid based on power-line signaling[J]. *IEEE Transactions on Industrial Electronics*, vol. 61, no. 7, pp: 3313-3326, 2014.
- [30] LIU X, WANG P, LOH P C. A hybrid AC/DC microgrid and its coordination control[J]. *IEEE Transactions on Smart Grid*, vol. 2, no. 2, pp. 278-286, 2011.
- [31] Yu Zhang, Nikolaos Gatsis, Georgios B. Giannakis. Robust energy management for microgrids with high-penetration renewables[J]. *IEEE Tran. Sustain Energy*, vol. 4, no. 4, pp. 944-953, Oct 2013

- [32] LU X N, GUERRERO J M, SUN K, et al. Hierarchical control of parallel AC-DC converter interfaces for hybrid microgrids[J]. IEEE Transactions on Smart Grid, vol. 5, no. 2, pp: 683-692, 2014.
- [33] Q. Hui, J. Yang, X. Yang, Z. Chen, Y. Li and Y. Teng, "A robust control strategy to improve transient stability for AC-DC interconnected power system with wind farms," CSEE Journal of Power and Energy Systems, vol. 5, no. 2, pp. 259-265, June 2019.
- [34] Zhou K, Doyle J C. Essentials of robust control[M]. New Jersey: Prentice Hall, 1999.
- [35] Attarha A, Amjady N, Conejo AJ. Adaptive robust AC optimal power flow considering load and wind power uncertainties. Int J Electr Power Energy Syst vol. 96, pp: 132-142, 2018
- [36] Gan W, Ai X, Fang J, Yan M, Yao W, Zuo W, et al. Security constrained co-planning of transmission expansion and energy storage. Appl Energy 2019; 239:383-394.
- [37] M. Zhou, M. Wang, J. F. Li, and G. Y. Li, "Multi-area generationreserve joint dispatch approach considering wind power cross-regional accommodation," CSEE Journal of Power and Energy Systems, vol. 3, no. 1, pp. 74–83, Mar. 2017.



**Yun Teng** received the Ph.D. degree in electrical engineering from the Shenyang University of Technology, Shenyang, China, in 2009. He joined the Shenyang University of Technology in 2010, where he is currently a Professor in electrical engineering. He is a standing director as the IEEE PES DC Distribution Network Technical

Subcommittee. His research interests include multi-energy system dispatching automation and smart grid control theory.

E-mail: [tengyun@sut.edu.cn](mailto:tengyun@sut.edu.cn)



**Peng Sun** is currently pursuing the Ph.D. degree at the school of Electrical Engineering, Shenyang University of Technology. His major research direction: Multi-energy system optimization operation and control, E-mail: [sygvsunpeng@163.com](mailto:sygvsunpeng@163.com)



**Ouyang Leng** received her Bachelor of Accounting degree from the North China Electric Power University, China, in 2009. She is currently working for the State Grid East Inner Mongolia Economic Research Institute. Her research interests include multi-energy system economic operation. E-mail: [175881948@qq.com](mailto:175881948@qq.com)



**Zhe Chen** received the B.Eng. And M.Sc. degrees from Northeast China Institute of Electric Power Engineering, Jilin City, China, and the Ph.D. degree from the University of Durham, Durham, U.K. He is a Full Professor with the Department of Energy Technology, Aalborg University,

Aalborg, Denmark, where he is the leader of Wind Power System Research program in the Department of Energy Technology. He is also the the Danish Principle Investigator for Wind Energy of Sino-Danish Centre for Education and Research. His research areas are power systems, power electronics and electric machines; and his main current research interests are wind energy and modern power systems. He has led many research projects and has authored or coauthored more than 400 publications in his technical field.

Dr Chen is a Fellow of the Institution of Engineering and Technology and a Chartered Engineer in the U.K. He is an editor of the IEEE TRANSACTIONS ON POWER SYSTEMS and an associate editor of the IEEE TRANSACTIONS ON POWER ELECTRONICS. E-mail: [zch@et.aau.dk](mailto:zch@et.aau.dk)



© 2020. Notwithstanding the ProQuest Terms and Conditions, you may use this content in accordance with the associated terms available at <https://ieeexplore.ieee.org/Xplorehelp/#/accessing-content/open-access>.